

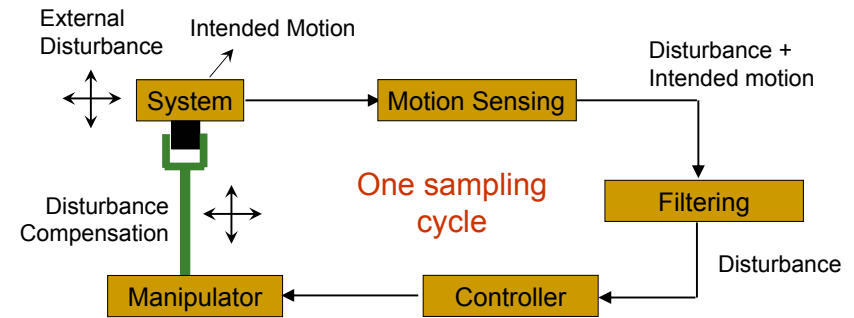
Active Tremor Compensation via Robotic Handheld Instrument and Wearable Orthosis

Wei Tech ANG

Assistant Professor
School of Mechanical and Aerospace Engineering
Nanyang Technological University, Singapore
wtang@ntu.edu.sg



Active Noise/Disturbance Compensation



- Low signal-to-noise ratio applications
 - Physiological tremor – micromanipulation
 - Pathological tremor – activities of daily living



Active Pathological Tremor Compensation in Wearable Orthosis

Wing Lok AU

Philippe POIGNET

Markus RANK (Exch Student)

Cheng Yap SHEE

Louis TAN

Adela TOW

Kalyana VELUVOLU

Ferdinan WIDJAJA

Dingguo ZHANG

National Neuroscience Institute

LIRMM, U of Montpellier II

Technische Universitaet Muenchen

Nanyang Technological University

National Neuroscience Institute

Tan Tock Seng Hospital

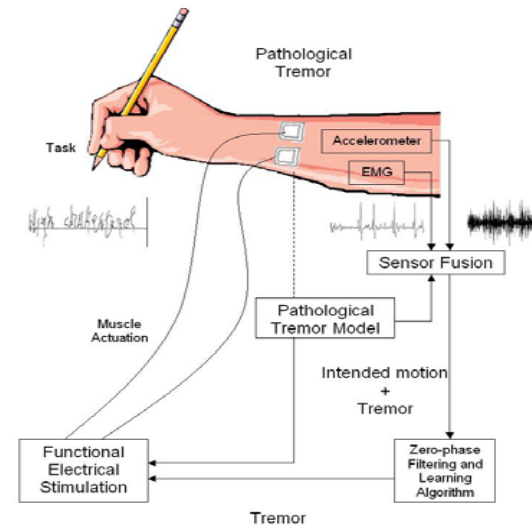
Nanyang Technological University

Nanyang Technological University

Nanyang Technological University



Active Pathological Tremor Compensation in Wearable Orthosis



Active Physiological Tremor Compensation in Handheld Microsurgical Instrument

David CHOI

Mingli HAN

Thiam Chye LIM

Yee Siang ONG

Cameron RIVIERE

Cheng Yap SHEE

U-Xuan TAN

Kalyana VELUVOLU

Tun Latt WIN

Carnegie Mellon University

Nanyang Technological University

National University Hospital

Singapore General Hospital

Carnegie Mellon University

Nanyang Technological University

Nanyang Technological University

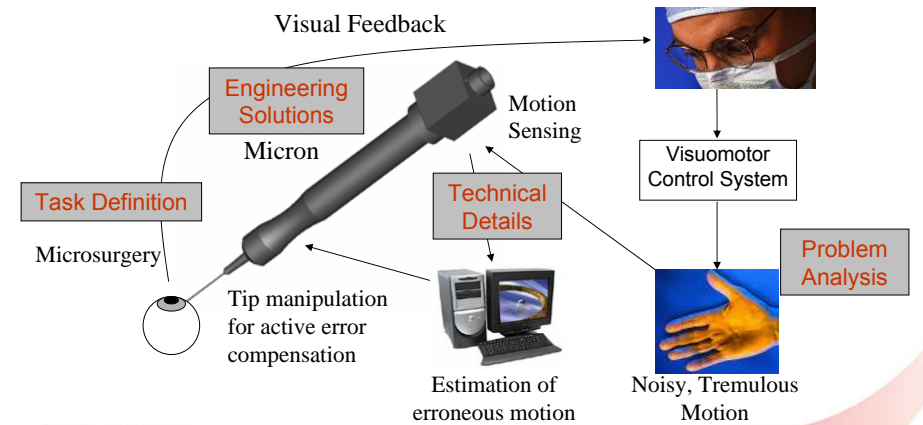
Nanyang Technological University

Nanyang Technological University



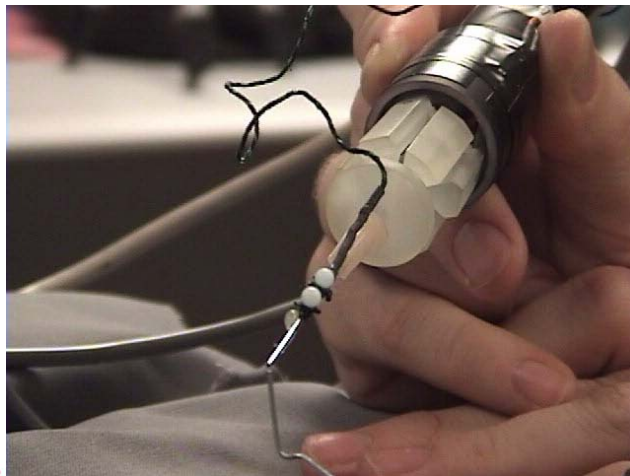
5

Microsurgery with Active Handheld Instrument



6

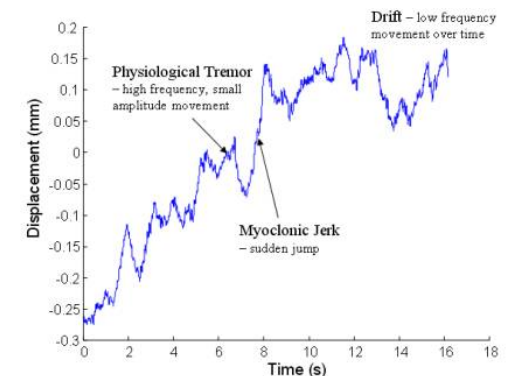
Active Physiological Tremor Compensation in Handheld Microsurgical Instrument



7

Involuntary Hand Movement for Healthy People

- Physiological Tremor
 - Roughly sinusoidal, $\leq 50 \mu\text{m rms}$, 8-12 Hz
- Others: Myoclonic jerk, drift



8

Physiological Tremor and Microsurgery

- Complicates microsurgical procedures and makes certain delicate interventions impossible



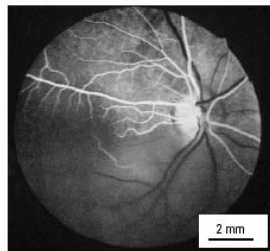
Vitreoretinal Microsurgery

- Removal of membranes $\leq 20 \mu\text{m}$ thick from front or back of retina

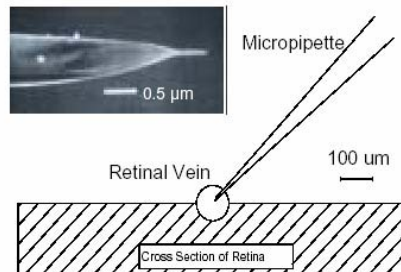


Vitreoretinal Microsurgery

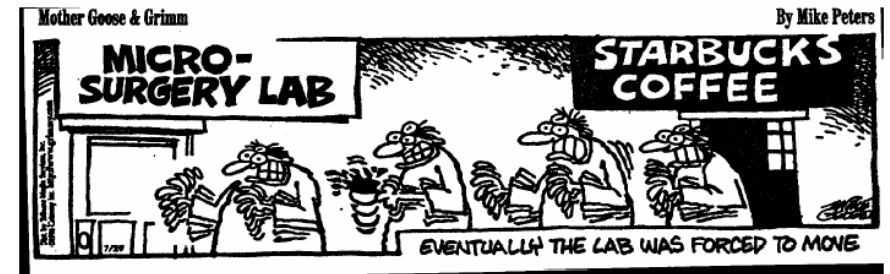
- Injection of anticoagulant using intraocular cannulation to treat retinal vein ($\sim \text{Ø}100 \mu\text{m}$) occlusion



Retina with occluded retinal vein



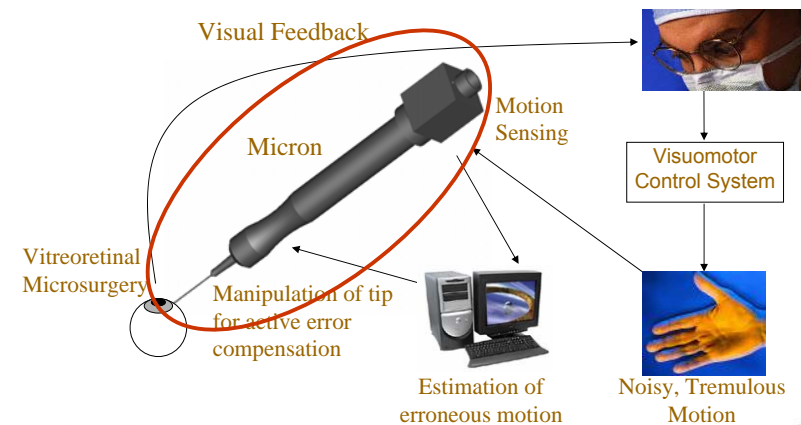
Physiological Tremor and Microsurgery



Physiological Tremor and Microsurgery

- Impact on microsurgeons
 - 2 of 10 surgeons become microsurgeons
- Factors affecting tremor
 - Fatigue – strenuous exercise etc.
 - Caffeine/alcohol consumption (withdrawal syndrome)
 - Lack of practice – long vacation etc.
 - Age – experience vs hand stability
- Microsurgeons' consensus:
 - 10 μm positioning accuracy

Microsurgery with Active Handheld Instrument



Comparison of Robotic Solutions

- | | |
|------------------------------|--------------------|
| | Obtrusive |
| ■ Telerobotics | > US\$1M |
| ■ 'Steady Hand' robot | > US\$150K |
| ■ Active Handheld Instrument | < US\$15K |
| | Unobtrusive |
-
- ✓ Cheap
 - ✓ Unobtrusive
 - ✓ Dexterity
 - × Limited workspace
 - × No motion scaling
 - × No 'third hand'

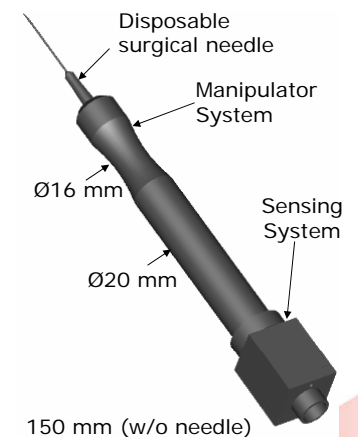


Da Vinci

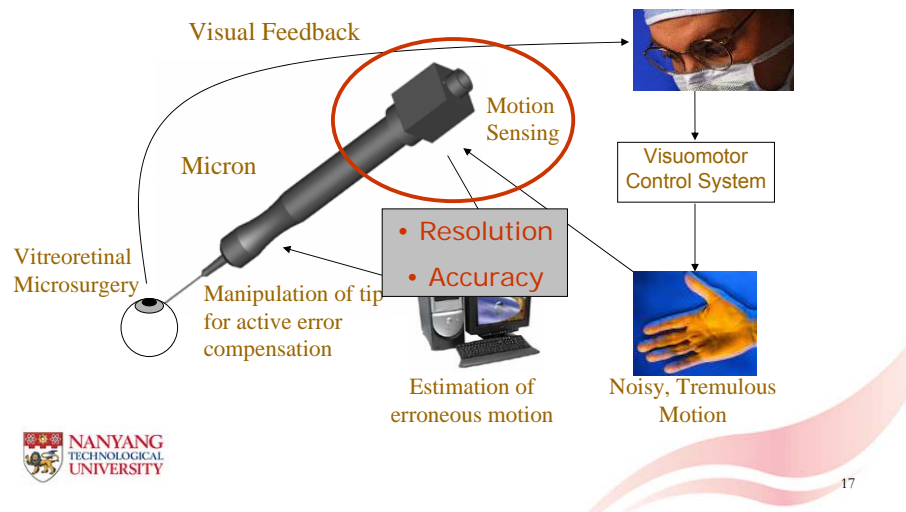
Steady Hand robot, Johns Hopkins Univ.

Micron Current Prototype

- Length: 150 mm long
- Diameter: $\text{Ø}20(16)$ mm
- Weight <100 g
- 6 DOF inertial at the back end
- 3 DOF piezoelectric driven parallel manipulator at front end with disposable surgical needle
- Signal processing and control performed by PC via ADC & DAC

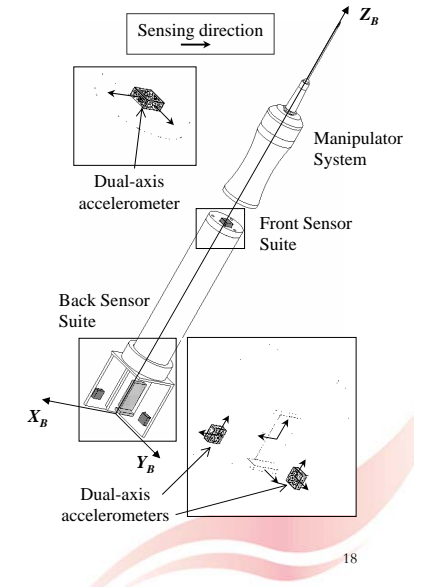


Microsurgery with Active Handheld Instrument



On-board Sensing System

- All-accelerometer inertial measurement unit (IMU):
 - 3 dual-axis miniature MEMS accelerometers Analog Devices ADXL-203: 5mm x 5mm x 2mm, < 1g
- Housed in 2 locations



Differential Sensing Kinematics

- Body acceleration sensed by accelerometer at location $\{i\}$:

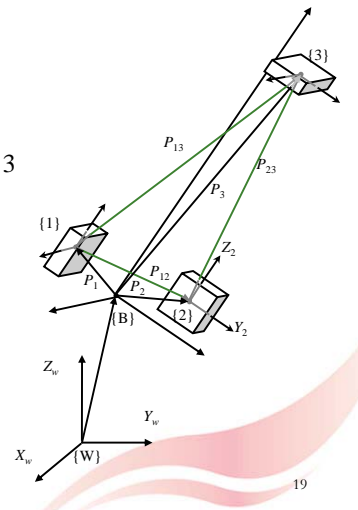
$$A_i = A_{CG} + g + \underbrace{\Omega \times \Omega \times P_{Bi} + \alpha \times P_{Bi}}_{\text{Rotation-induced Accelerations}}$$

- Differential Sensing

$$A_{ij} = A_j - A_i = ([\Omega \times][\Omega \times] + [\alpha \times])P_{ij}, i, j = 1, 2, 3$$

$$A_{13} = \begin{bmatrix} a_{13x} \\ \bullet \\ \bullet \end{bmatrix}, A_{23} = \begin{bmatrix} \bullet \\ a_{23y} \\ \bullet \end{bmatrix}, A_{12} = \begin{bmatrix} \bullet \\ \bullet \\ a_{12z} \end{bmatrix}$$

- Solve system of nonlinear equations for $\Omega = [\omega_x \ \omega_y \ \omega_z]^T$ by Gauss-Newton or Levenberg-Marquart method



Sensing Kinematics

- Updating quaternions:

$$\dot{q}(t) = \tilde{\Omega}(t)q(t), \quad \tilde{\Omega} = \frac{1}{2} \begin{bmatrix} [\Omega \times]_{3 \times 3} & \Omega_{3 \times 1} \\ -\Omega_{1 \times 3}^T & 0 \end{bmatrix}$$

- Directional Cosines matrix

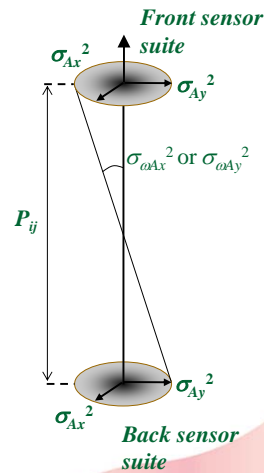
$${}^W C_B = \begin{bmatrix} q_0^2 + q_1^2 - q_2^2 - q_3^2 & 2(q_1q_2 - q_0q_3) & 2(q_1q_3 + q_0q_2) \\ 2(q_1q_2 + q_0q_3) & q_0^2 - q_1^2 + q_2^2 - q_3^2 & 2(q_2q_3 - q_0q_1) \\ 2(q_1q_3 - q_0q_2) & 2(q_2q_3 + q_0q_1) & q_0^2 - q_1^2 - q_2^2 + q_3^2 \end{bmatrix}$$

- Gravity Removal: ${}^W A_E = {}^W C_B {}^B A - {}^W g$
- Tip Displacement:

$${}^W P_{tip}(t) = {}^W P_{tip}(t-T) + \int_{t-T}^t \int {}^W A_E(\tau) d\tau d\tau + {}^W C_B(t) [{}^B \Omega \times] {}^B P_{tip}$$

Sensing Resolution (Error Variance) Analysis

- Sensing resolution dependent on sensor noise floor
- Angular Sensing
 - Sensing equation:
 $A_{ij} = f(\Omega) = ([\Omega \times] [\Omega \times] + [\alpha \times]) P_{ij}$
 - Covariance:
 $C(A_{ij}) = C(\Omega) P_{ij}$
 - $P_{ij} \uparrow, C(\Omega) \downarrow$



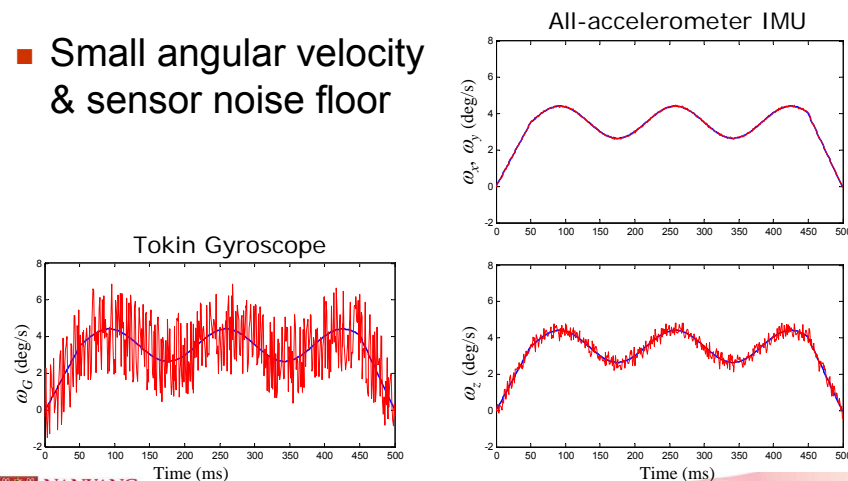
Proposed All-Accelerometer vs Conventional Inertial Measurement Unit

- All-accelerometer IMU
 - Maximized P_{ij} with physical constraint of a slender handheld instrument
- Conventional IMU (3A-3G)
 - Tokin CG-L43D rate gyros x 3

	3G-3A Error std. dev. (deg/s)	6A Error std. dev. (deg/s)	Noise reduction / resolution improvement
ω_x & ω_y	1.41	1.08×10^{-2}	99.3% / 130x
ω_z	1.41	4.42×10^{-2}	96.9% / 32x

Angular Sensing Resolution Comparison

- Small angular velocity & sensor noise floor



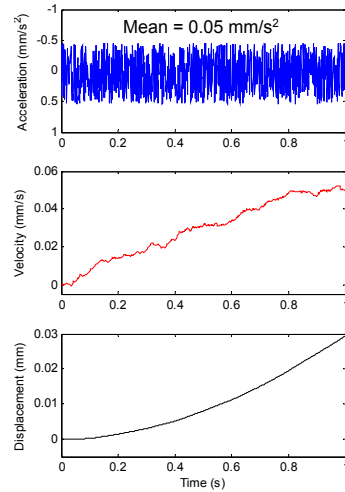
Sensing Resolution (Error Variance) Analysis

- Translational Sensing
 - 2 accelerometers in each sensing direction:

$$\frac{1}{\sigma_A^2} = \frac{1}{\sigma_{Ai}^2} + \frac{1}{\sigma_{Aj}^2} \rightarrow \sigma_A = \frac{\sigma_{Ai}}{\sqrt{2}}$$
 - Sensing resolution improves by a factor of $\sqrt{2}$
- Better orientation estimation \rightarrow more complete removal of gravity \rightarrow better translation estimation

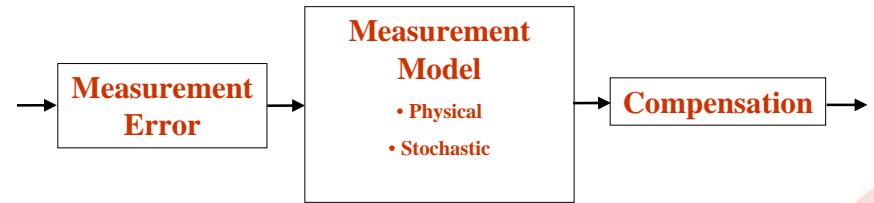
Integration Drift of Inertial Sensors

- Integration drift
 - Erroneous DC Offset
 - Ramp →
 - Quadratic
 - Error accumulates and grows unbounded over time
- Poor sensing accuracy

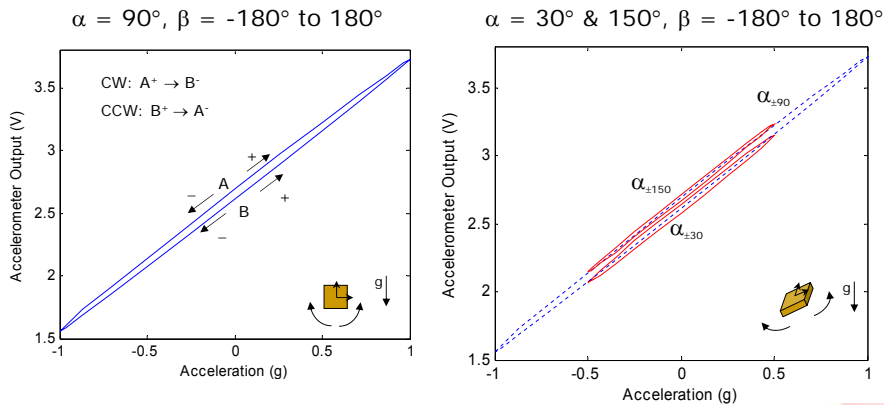


Measurement Model

- Measurement model allows error analysis and compensation
- Measurement Model = Physical (Deterministic) Model + Stochastic Model

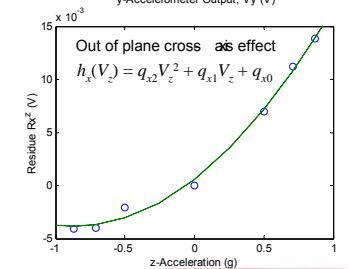
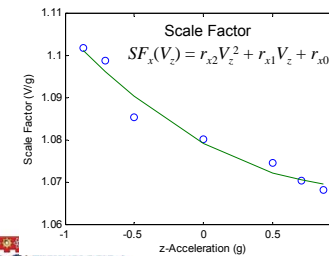
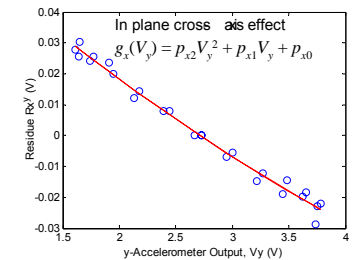


Experimental Observations



Phenomenological Modeling

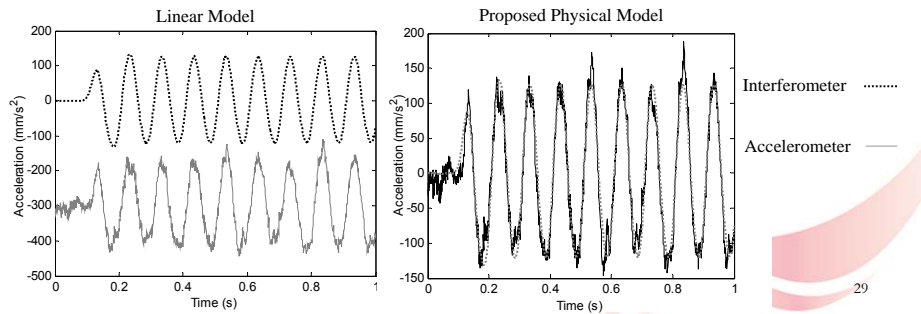
- Bias, $B_x(V_y, V_z) = B_x + g_x(V_y) + h_x(V_z)$
- Scale Factor,
 $SF_x(V_z) = r_{x2}V_z^2 + r_{x1}V_z + r_{x0}$
- Model
 $A_x = (V_x - B_x(V_y, V_z)) / SF_x(V_z)$



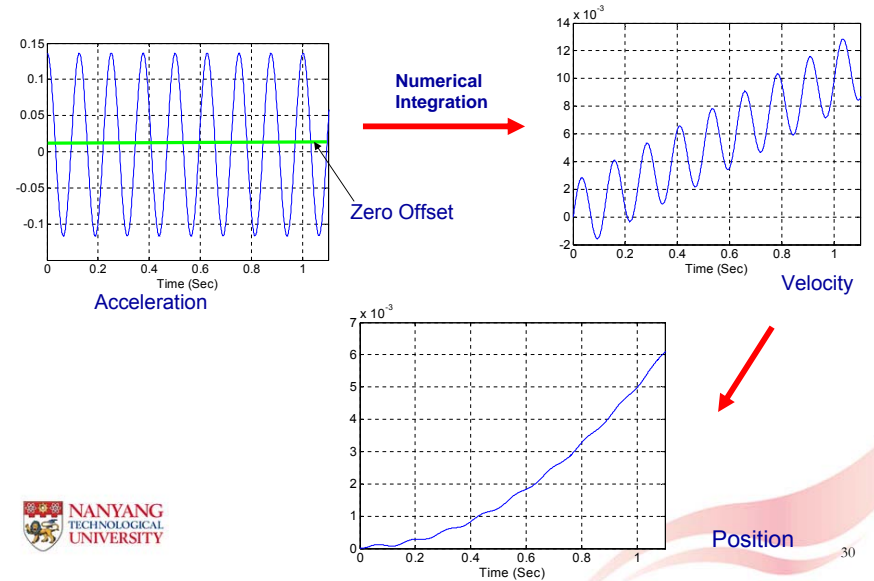
Sensing Results - Translation

	Rmse (mm/s ²)	Bias (mm/s ²)	Scale Factor (mm/s ²)
Linear Model	300	272	6
Proposed Physical Model	31*	<5	<1
Error Reduction (%)	89.7	-	-

* ADXL-203 rated rms noise = 22.1 mm/s²



Residual Zero Offset - Integration Drift



Analytical Integration

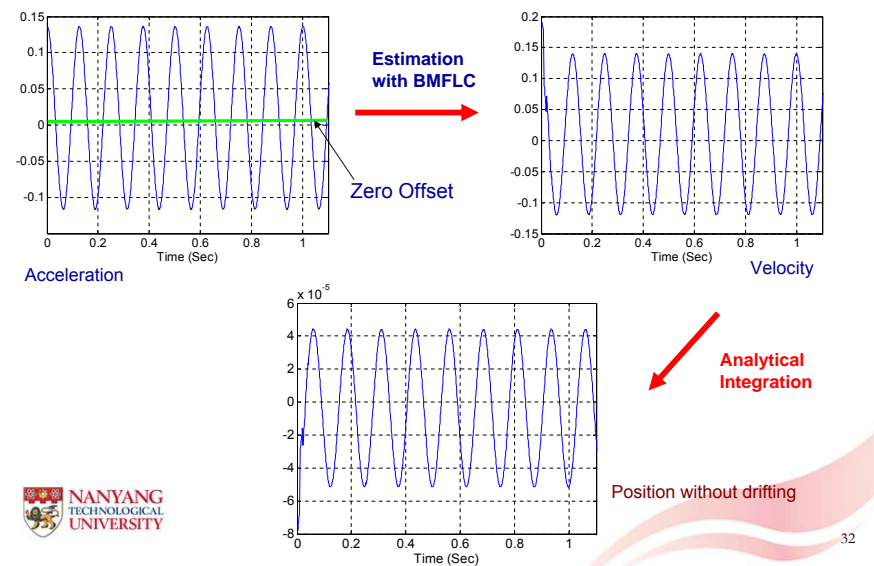
Real-time modeling of Tremor

$$\text{Acceleration: } y_k = \sum_{r=0}^{L=(f-f_0)G} a_r \sin(2\pi(f_0 + \frac{r}{G})k) + b_r \cos(2\pi(f_0 + \frac{r}{G})k)$$

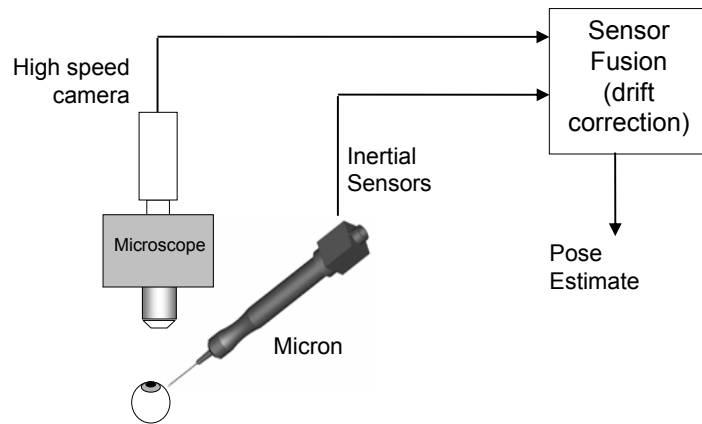
$$\text{Velocity: } \int y_k = -\sum_{r=0}^L \left[\frac{a_r}{(2\pi(f_0 + \frac{r}{G}))} \cos(2\pi(f_0 + \frac{r}{G})k) - \frac{b_r}{(2\pi(f_0 + \frac{r}{G}))} \sin(2\pi(f_0 + \frac{r}{G})k) \right]$$

$$\text{Position: } \iint y_k = -\sum_{r=0}^L \left[\frac{a_r}{(2\pi(f_0 + \frac{r}{G}))^2} \sin(2\pi(f_0 + \frac{r}{G})k) + \frac{b_r}{(2\pi(f_0 + \frac{r}{G}))^2} \cos(2\pi(f_0 + \frac{r}{G})k) \right]$$

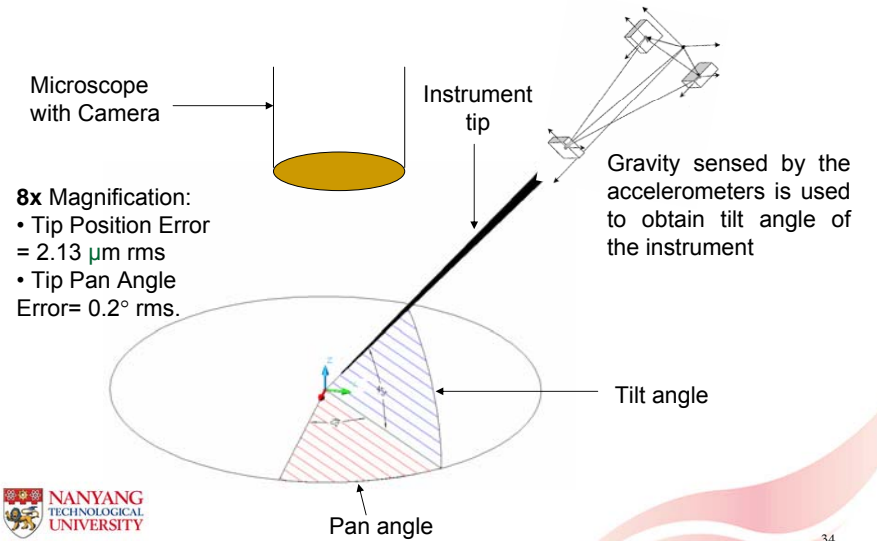
Analytical Integration



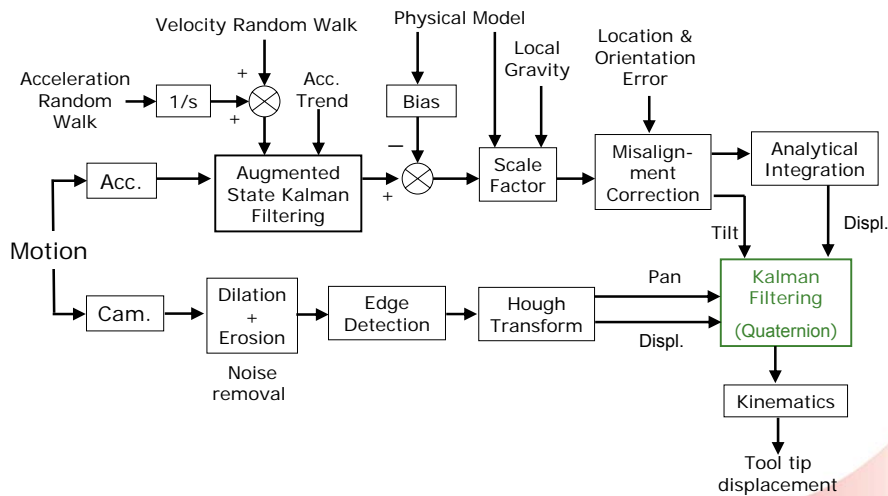
Vision Aided Inertial Sensing



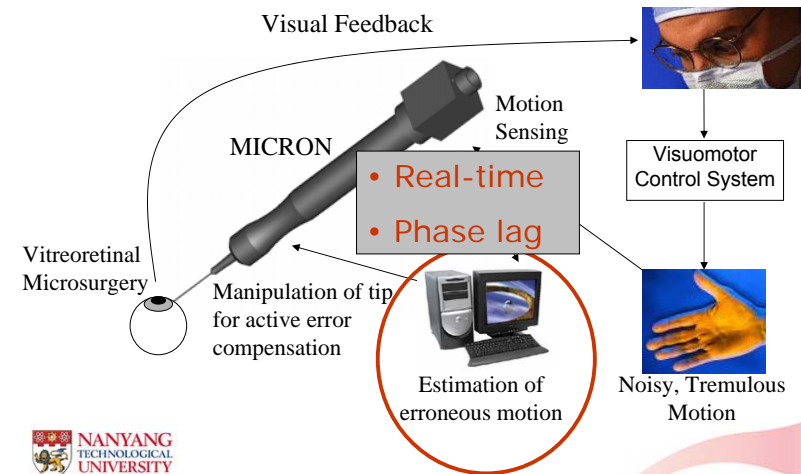
Vision Aided Inertial Sensing



Sensor Fusion



Microsurgery with Active Handheld Instrument

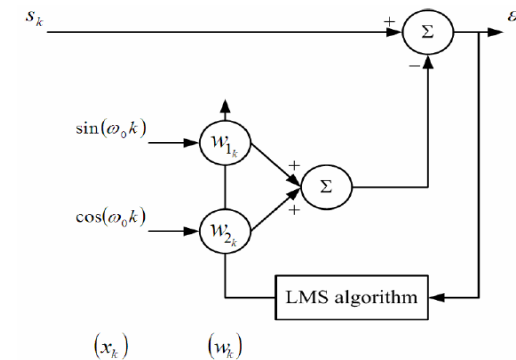


Zero Phase Filtering

- Phase lag = time delay
- Separation of tremor from the intended motion without introducing phase lag
 - Prediction/projection capability
 - Adaptive
 - Non-linear phase response of IIR filter, i.e. phase characteristic changes with frequency

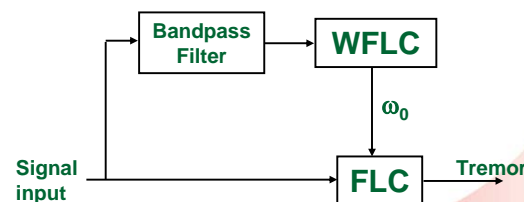
Fourier Linear Combiner (FLC)

- Truncated Fourier series to adaptively estimate amplitude and phase of periodic signal with *known frequency* (ω_0)

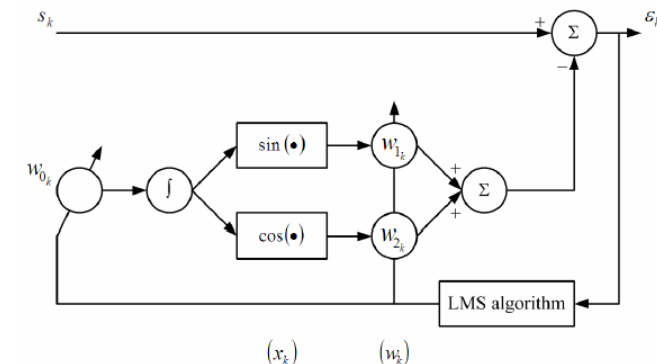


Weighted-frequency Fourier Linear Combiner (WFLC)

- Extends FLC to also adaptively estimate the frequency using another LMS algorithm
- Band-pass filter to select the band of interest
 - Assumption: rate of change of the dominant input signal frequency is slow
- Zero-phase notch (band-stop) filter effect

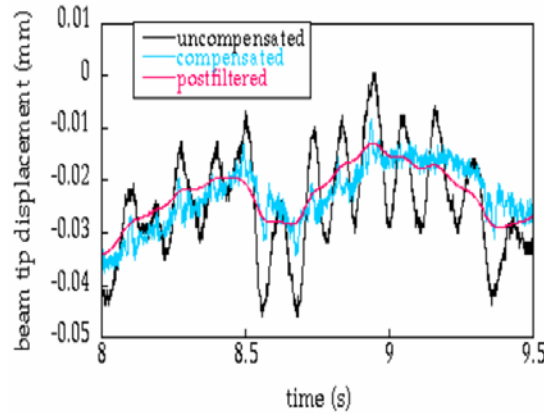


Weighted-frequency Fourier Linear Combiner (WFLC)

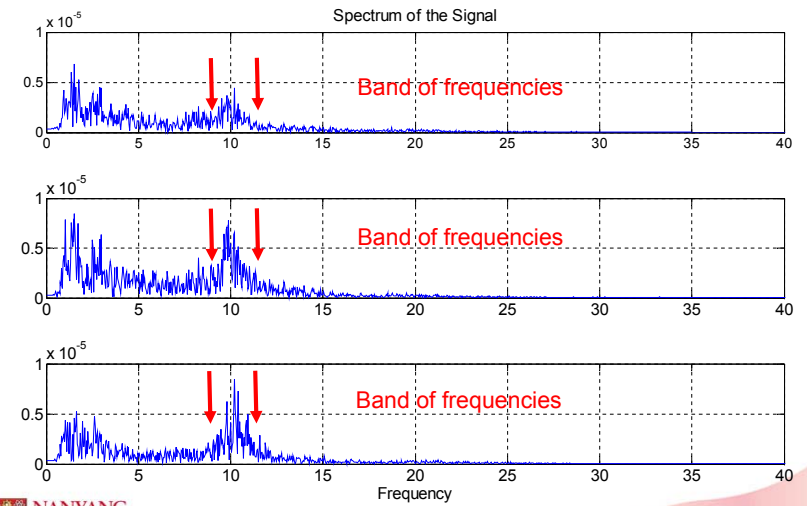


Weighted-frequency Fourier Linear Combiner (WFLC) Experiment

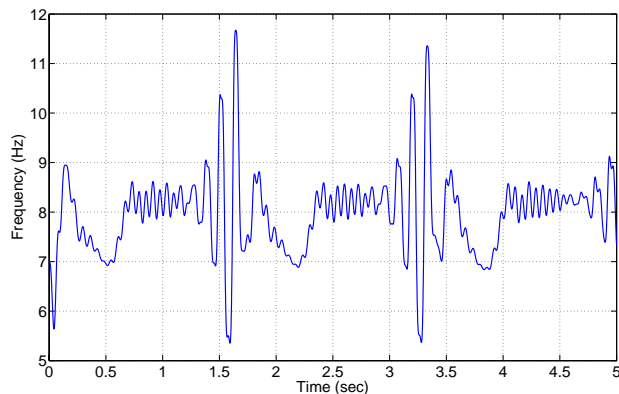
- 1 DOF motion canceling experiment
- Ave. rms tremor amplitude reduced 69%



Tremor Recordings



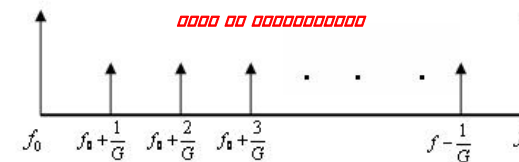
Frequency adaptation in WFLC



The frequency adaptation becomes unstable due to the presence of two frequencies 8 & 8.6 Hz

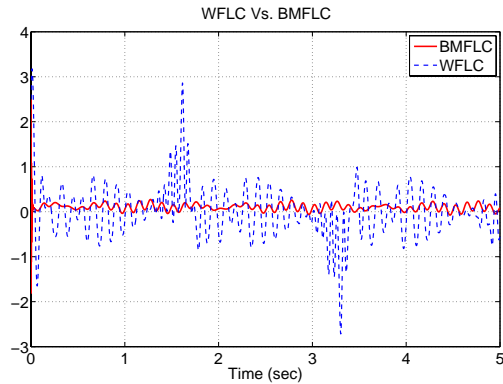
Bandlimited Multiple FLC

- To estimate the tremor signal within a band of frequencies or comprising of multiple frequency components (modulated signals)



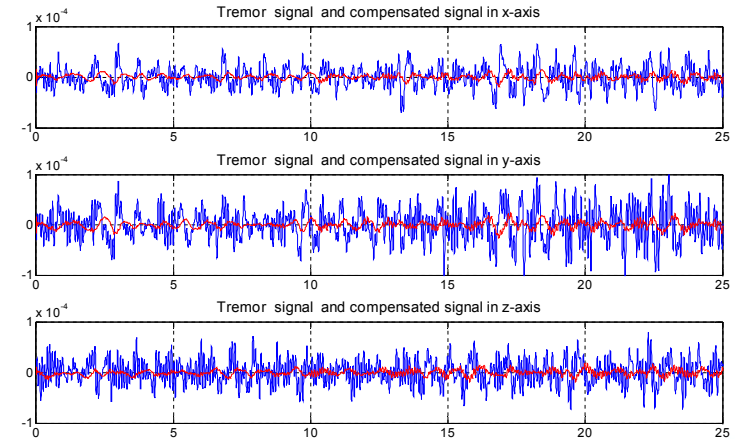
- Corresponding weight will adapt to the corresponding frequency of the input signal
- Can deal with input signals of multiple frequency components unlike WFLC

Comparative Performance : Estimation Errors



Presence of two frequencies 8 and 8.6 degrades the performance of WFLC

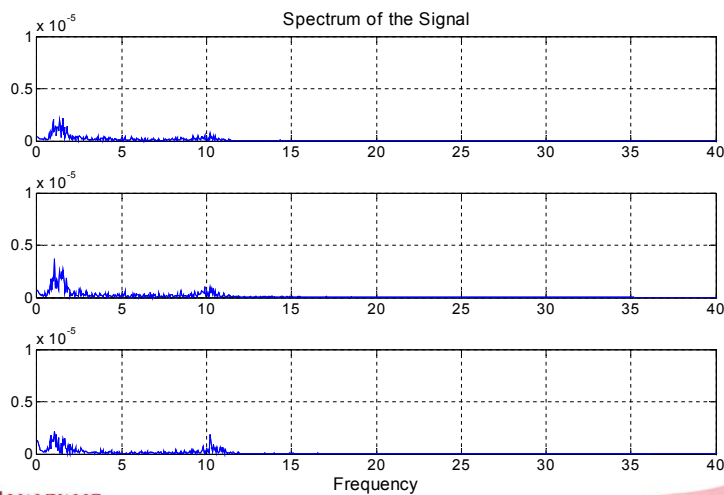
Performance of BMFLC with Real-Tremor



Red line shows the compensated motion

Band of BMFLC: 3- 12 Hz.

Performance of BMFLC with Real-Tremor



Spectrum of the compensated motion.

Analytical Integration via BMFLC

- Frequency components remain constant in BMFLC
- Once the weights adapt, the weights can also be assumed to be constant

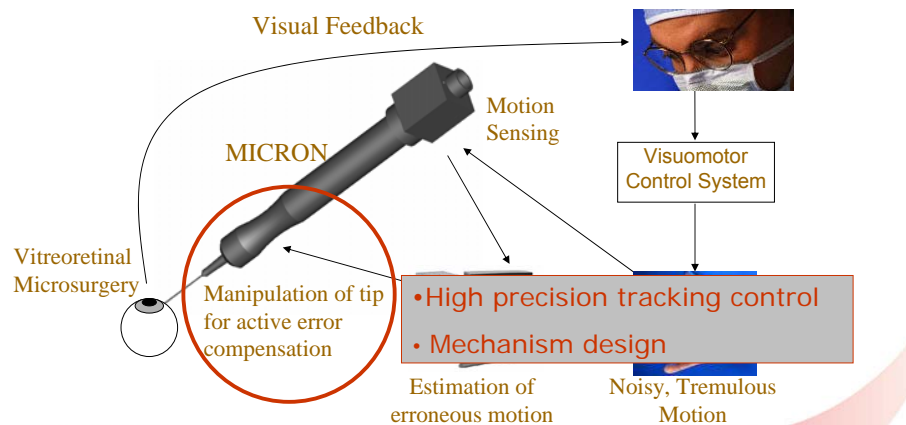
By Performing analytical integration:

$$\text{Acceleration: } y_k = \sum_{r=0}^{L=(f-f_0)G} a_r \sin(2\pi(f_0 + \frac{r}{G})k) + b_r \cos(2\pi(f_0 + \frac{r}{G})k)$$

$$\text{Velocity: } \int y_k = -\sum_{r=0}^L \left[\frac{a_r}{(2\pi(f_0 + \frac{r}{G}))} \cos(2\pi(f_0 + \frac{r}{G})k) - \frac{b_r}{(2\pi(f_0 + \frac{r}{G}))} \sin(2\pi(f_0 + \frac{r}{G})k) \right]$$

$$\text{Position: } \iint y_k = -\sum_{r=0}^L \left[\frac{a_r}{(2\pi(f_0 + \frac{r}{G}))^2} \sin(2\pi(f_0 + \frac{r}{G})k) + \frac{b_r}{(2\pi(f_0 + \frac{r}{G}))^2} \cos(2\pi(f_0 + \frac{r}{G})k) \right]$$

Microsurgery with Active Handheld Instrument

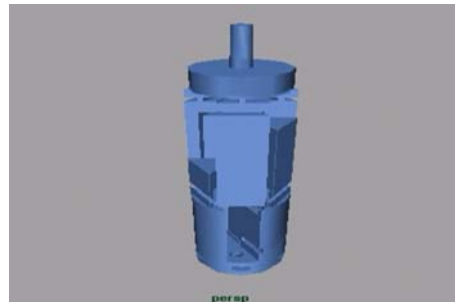


Manipulator Design

- 3 DOF piezoelectric-driven parallel manipulator
 - 1 actuator per axis, max effective stroke = $12.5 \mu\text{m}$
 - Motion amplification = $9.4x$, total stroke $> 100 \mu\text{m}$
- Tool tip approximated as a point, hence only 3 DOF manipulation
- Parallel manipulator design because
 - Rigidity, compactness, and design simplicity

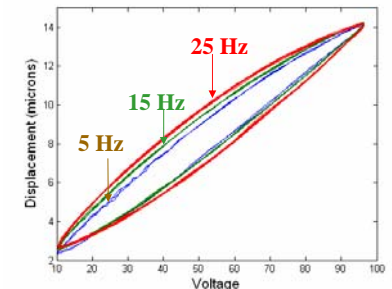
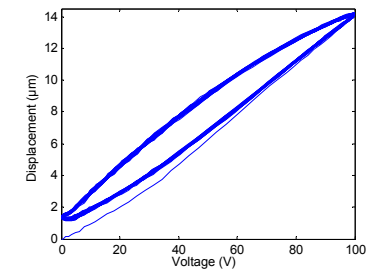
Design of Parallel Mechanism

- Flexure Based Mechanism
- Monolith design using Stereolithography (SLA)
- $\varnothing 22 \times 58 \text{ mm}$
- IEEE EMBS 2005 (Shanghai) Best Student Design Competition winner
 - David Choi (CMU) et al.



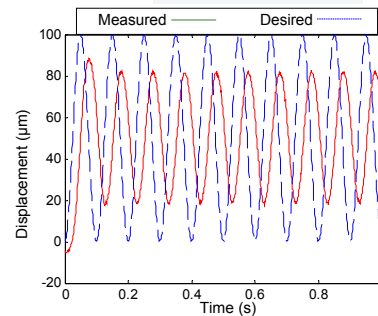
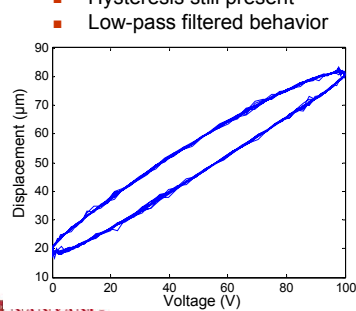
Piezoelectric Actuator Hysteresis

- Pros :
 - High bandwidth
 - Fast response
 - High output force
- Cons :
 - Hysteresis
- $\sim 15\%$ of max. displacement
- Hysteresis is rate-dependent



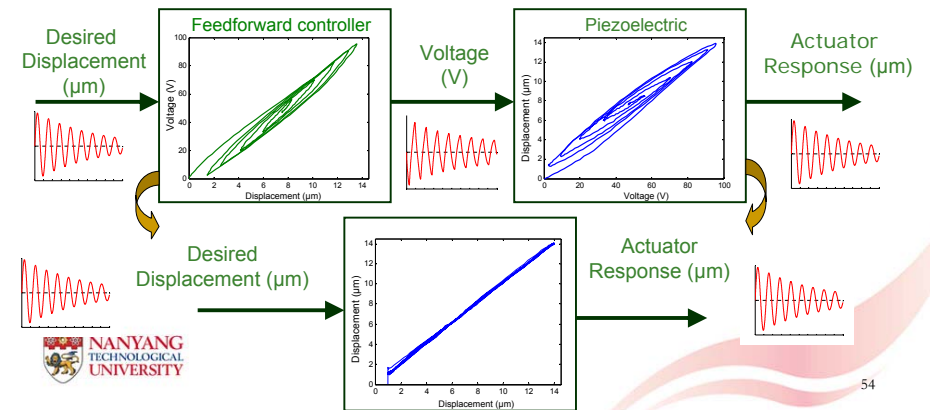
Commercial Piezo-System with Feedback Controller

- Piezo-driven 3 axis micro-positioner
 - Polytec-PI, Germany, NanoCube™ P-611
 - >\$ 10,000
 - Feedback sensors: strain gages
 - Tracking a 10 Hz, 100 μm p-p sinusiod
 - Hysteresis still present
 - Low-pass filtered behavior



Feedforward Controller with Inverse Hysteresis Model

- Develop an invertible mathematical model that closely describes the hysteretic behavior of a piezoelectric actuator
- Prandtl-Ishlinskii Model

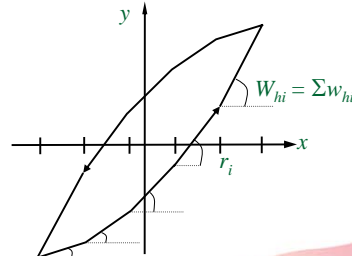
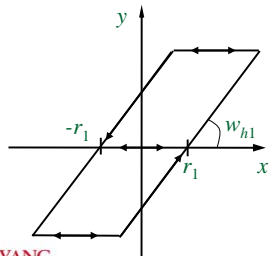


Prandtl-Ishlinskii (PI) Operator

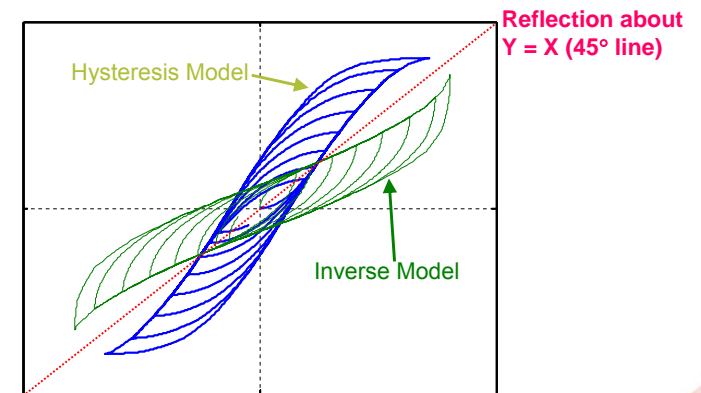
- Rate independent backlash operator:

$$H_r = \max\{x(t) - r, \min\{x(t) + r, y_0\}\}$$
- Linearly weighted superposition of backlash operators:

$$y(t) = \vec{w}_h^T \vec{H}_r[x, \vec{y}_0](t)$$

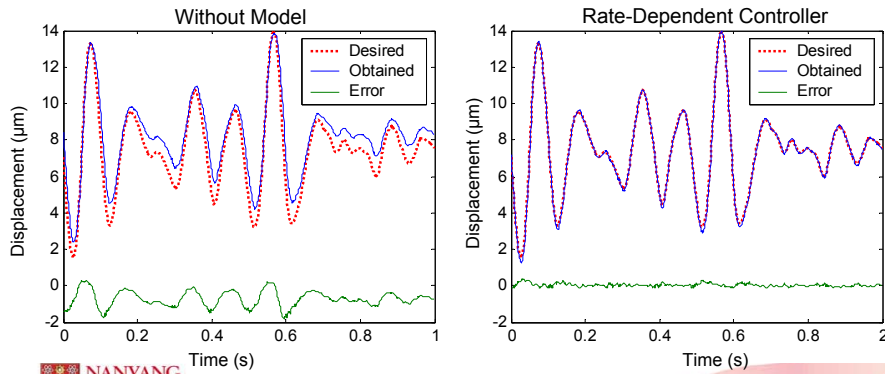


Inverse PI Hysteresis Model



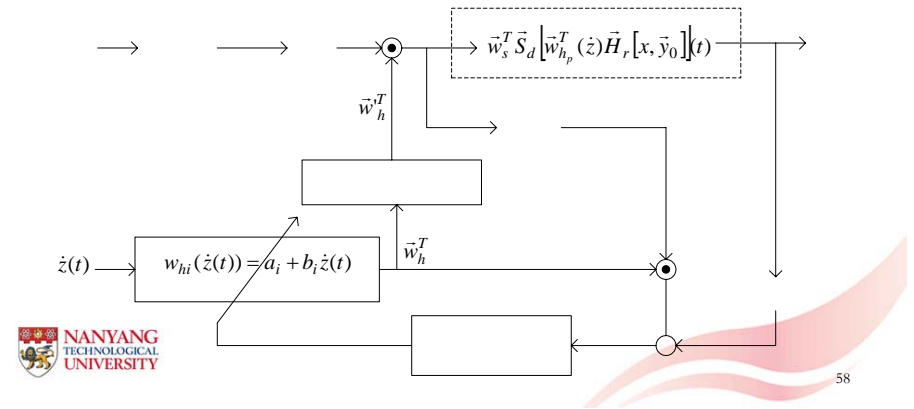
Tremor Tracking Results

- Tracking recordings of real tremor using 1 piezoelectric stack
 - Rmse = 0.64% of max ampl.; Max error = 2.4% of max ampl.

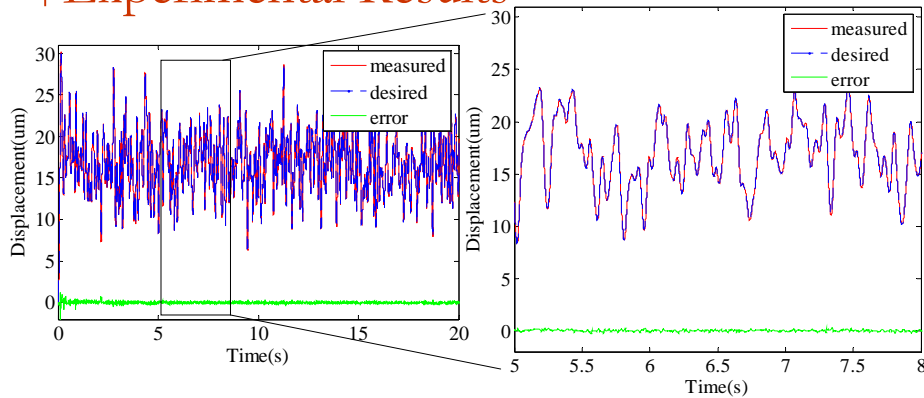


Adaptive Feedforward Controller

- Eliminate parameter identification
- Weight adapting mechanism: Recursive Least Square

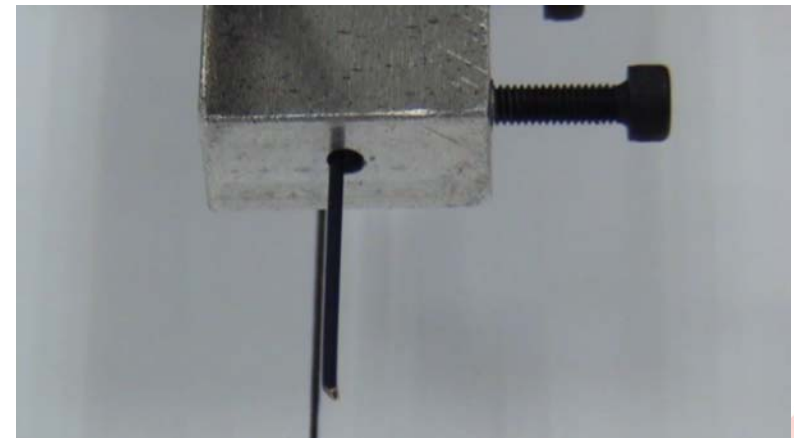


Experimental Results



	Adaptive Rate-dependent Controller
rmse $\pm \sigma$ (μm)	0.0943 ± 0.0159
rmse / actuator's stroke length (%)	0.31
max error $\pm \sigma$ (μm)	0.3899 ± 0.0291
max error / actuator's stroke length (%)	1.30

Real-time Active Compensation – 1 DOF Disturbance, 1 DOF Compensation



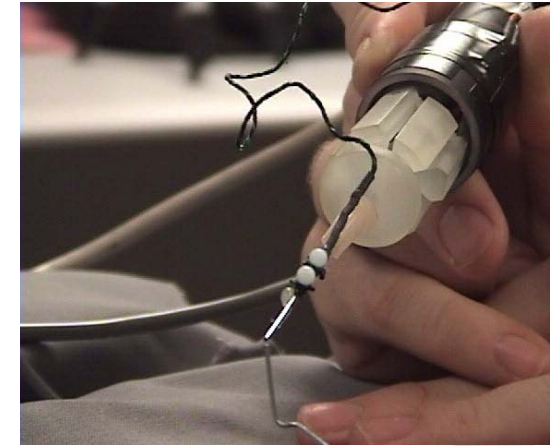
y_d

Real-time Active Compensation – 1 DOF Disturbance, 3 DOF Compensation

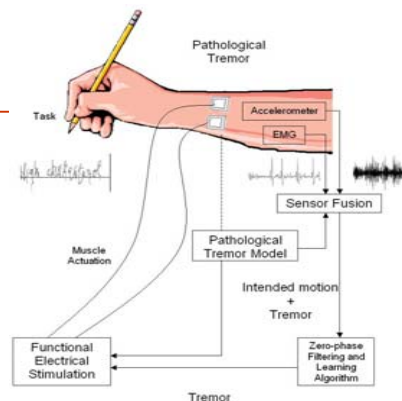


Real-time Active Compensation – Handheld

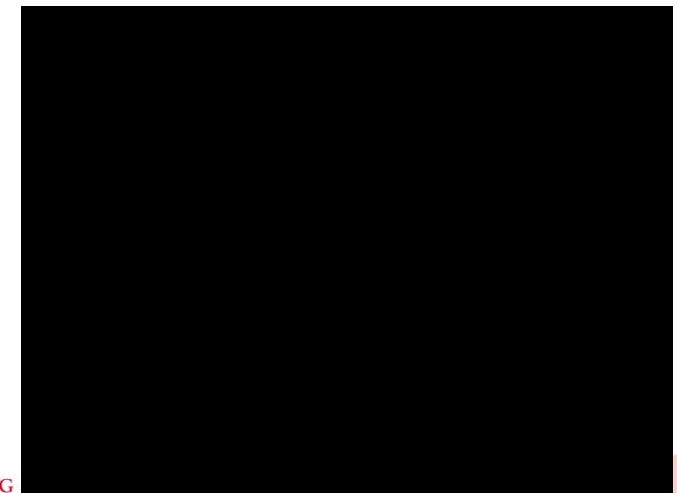
- C. Riviere (2006), Carnegie Mellon Univ.
- 5 DOF sensing by 2 orthogonal position sensitive detectors
- No inertial sensing
- Non-surgical scenario



Active Pathological Tremor Compensation in Wearable Orthosis

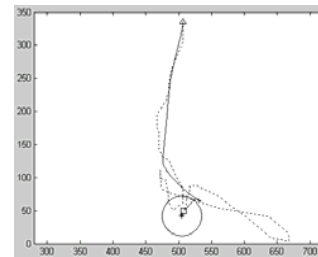


Pathological Tremor



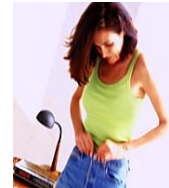
Pathological Tremor: Causes & Symptoms

- 3-12 Hz
- From < 10 mm (fingers) to > 100 mm (arm)
- Common medical conditions
 - Essential tremor (postural tremor)
 - Parkinson's disease (resting tremor)
 - Cerebellar dysfunction (intention tremor)
 - e.g. stroke, multiple sclerosis, Wilson's disease



Impact of Pathological Tremor

- Affects 5-9% of the population age ≥ 40
- Activities of daily living become challenging or impossible



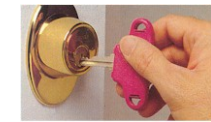
buttoning



writing



typing



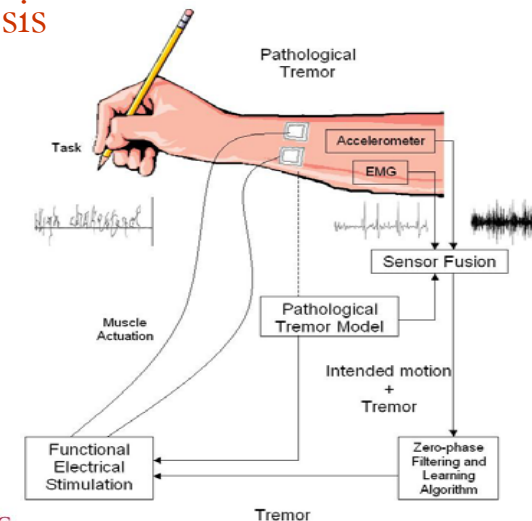
Inserting a key

- Social embarrassment and isolation
- Lifetime cost per patient > US\$1M

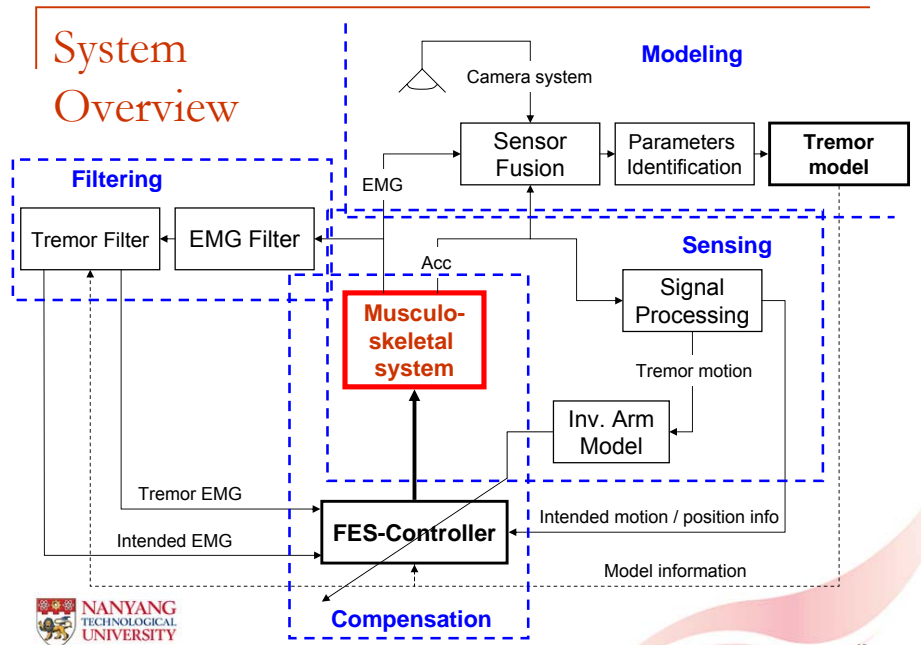
Treatment Options

- Drug therapy
 - > 50% are not responsive to drug
- Stereotactic surgery
 - Cost, psychological barrier, chances of complication
- Assistive technology
 - Active tremor compensation via wearable orthosis
 - A 20-100 ms electromechanical time delay between Electromyograph (EMG) signals and muscle actuations

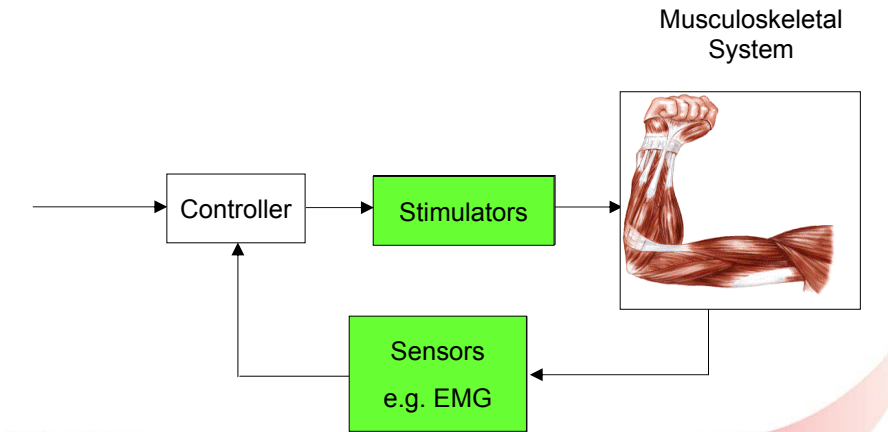
Active Tremor Compensation in Wearable Orthosis



System Overview



Feedback Control System

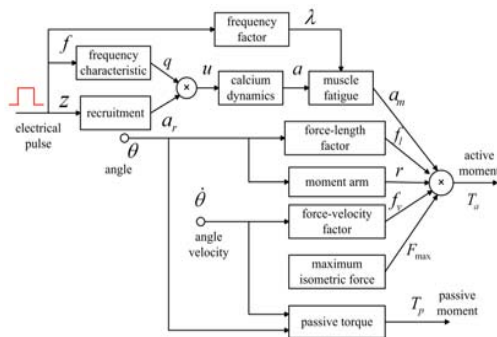


Robot Arm vs Human Arm - Actuation system

$$T_m = K_t i$$

$$e = K_t \omega_m$$

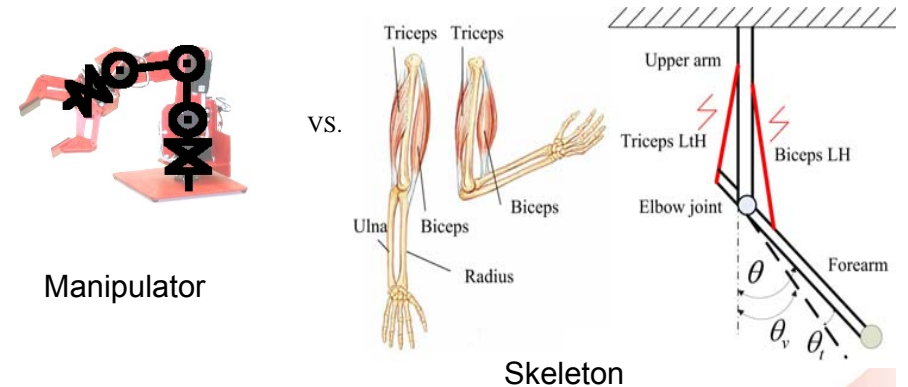
$$V_a = iR + L \frac{di}{dt} + e$$



Electrical Motor

Muscle (Hill-Type)

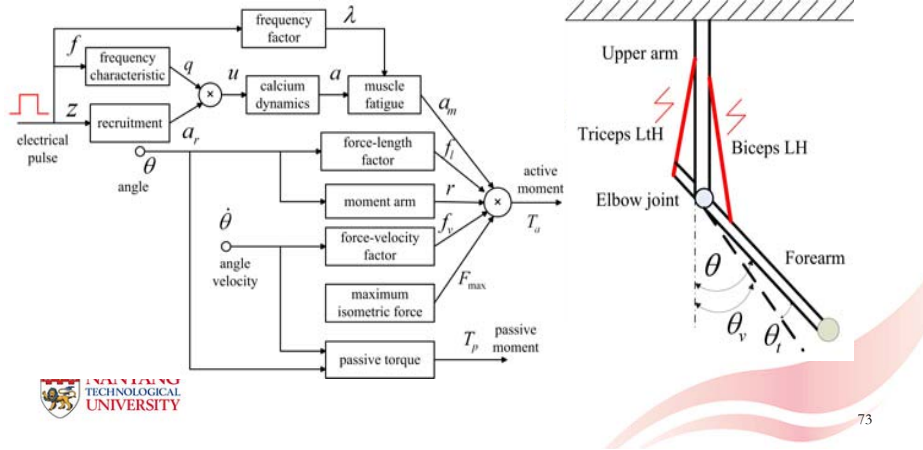
Robot Arm vs Human Arm - Links



Kinematics & Dynamics are solved in similar ways

Musculoskeletal Model of Upper Limb

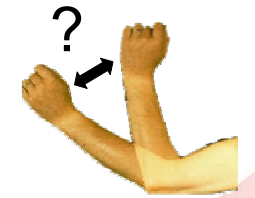
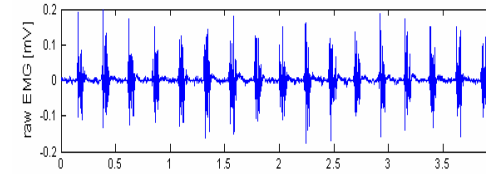
- Well studied and established



Key Challenges

- Sensing

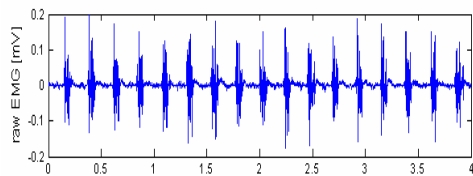
- How can we know what upper limb movement (tremulous + voluntary) will occur from the sensed SEMG of the muscles?



Key Challenges

- Filtering

- How can we differentiate between tremulous & voluntary SEMG of the muscles?



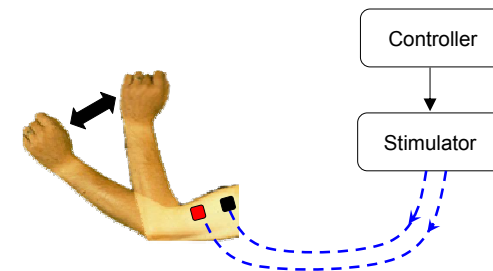
Tremor

Intended Movement

Key Challenges

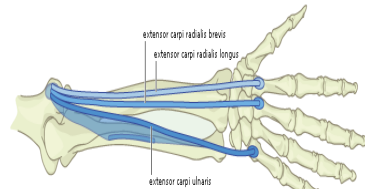
- Functional Electrical Stimulation

- How can we use FES to generate (anti-)tremulous movement in the upper limbs?

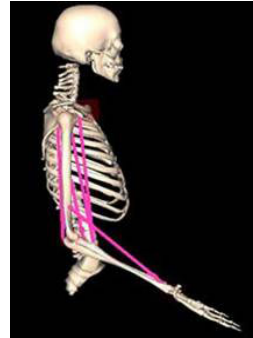


Musculoskeletal Modeling of Tremor in Upper Limbs

- To understand the roles and characteristics of the skeletal muscles responsible for each type of tremor
- To study SEMG-movement relationship



Copyright © 2012, William Scavone

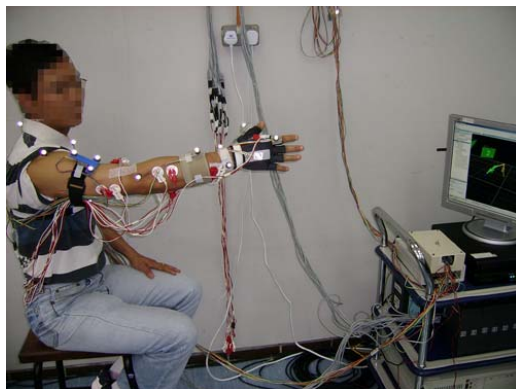


Tremor Study

- 120 patients with movement disorder
 - Parkinson Diseases – resting tremor (>30)
 - Essential Tremor – postural tremor (>30)
 - Multiple Sclerosis, Stroke, etc. – intention tremor (>30)
 - Others (~10)
- 30 healthy people
 - Age 16-85
 - No personal & family medical history of tremor
- National Neuroscience Institute, Singapore

Pathological Tremor Study

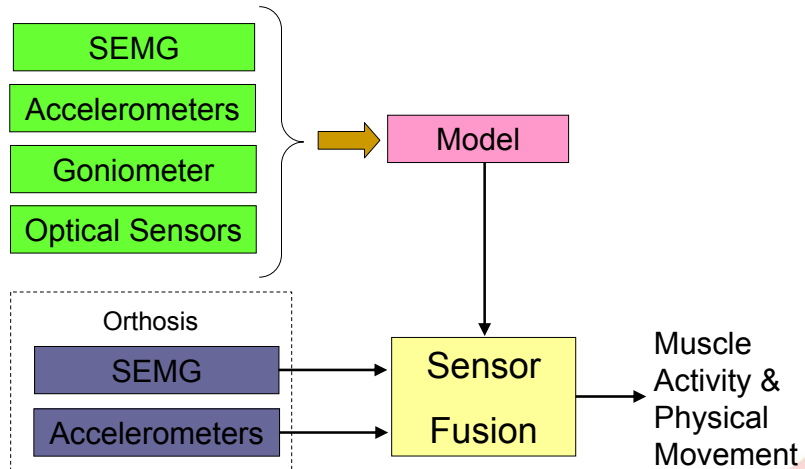
- 18 control subjects, 5 Parkinson's Disease patients, 6 Essential Tremor patients, 1 Psychogenic tremor patient, and 1 Holmes' tremor patient



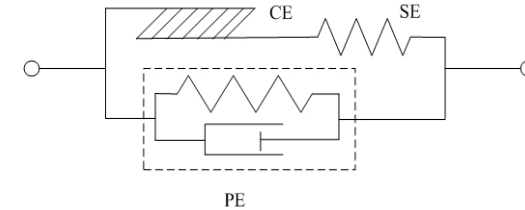
Data Collection

- Record sensor data of patients performing
 - Standard diagnostics: finger to nose, finger to finger, stretched out, drawing spirals, etc.
- Sensors
 - SEMG: 16 channels (8 muscle groups, mostly agonist & antagonist pairs) per limb
 - Accelerometers: 3 x tri-axial per limb
 - Goniometers: 1 per limb
 - Position and Orientation sensor: Vicon optical sensing system (4 cameras)

Sensing



Muscle Contraction Property



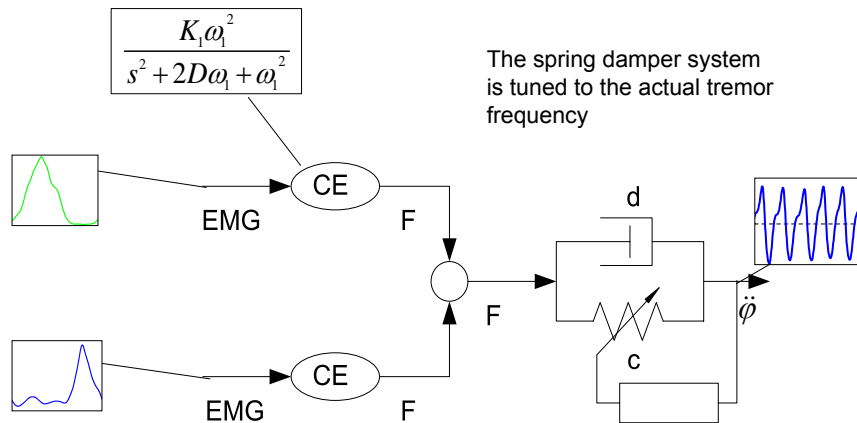
Muscle mechanical model (Hill-type)

CE : Contractile Element

SE : Series Elastic Element

PE : Passive Element (Parallel Elastic Element)

Phenomenological Modeling of Upper Limb Tremor from EMG



Sensor Fusion – Kalman Filtering

- EMG-derived joint angle as predictor
- ACC-derived joint angle as corrector

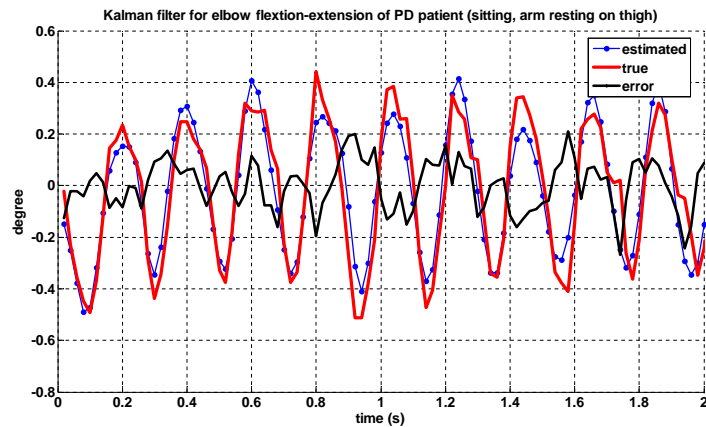
$$\theta_{EMG}(k) = c_{EMG}(1)EMG(k) + c_{EMG}(2)$$

$$\theta_{ACC}(k) = c_{ACC}(1)ACC(k) + c_{ACC}(2)$$

- Estimate of joint angle

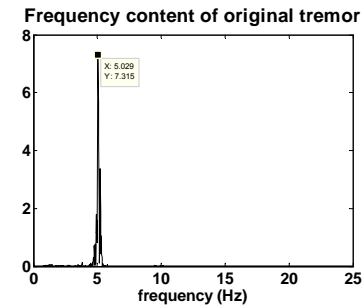
$$\theta(k) = \theta_{EMG}(k) + \frac{\sigma_{EMG}^2}{\sigma_{EMG}^2 + \sigma_{ACC}^2} (\theta_{ACC}(k) - \theta_{EMG}(k))$$

Results

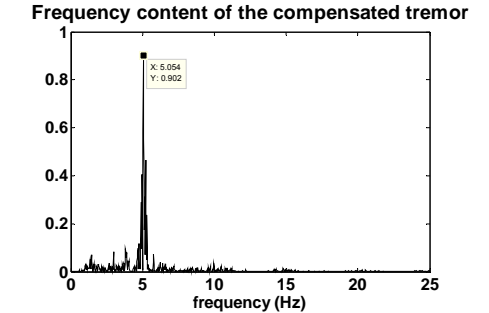


$\sigma^2_{\text{true}} = 0.1045$
 $\sigma^2_{\text{error}} = 0.022$ (78.76% reduction)

Results



Power of original tremor = 7.315

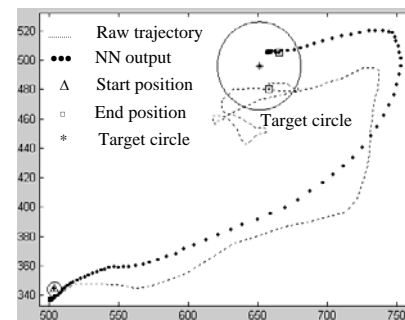
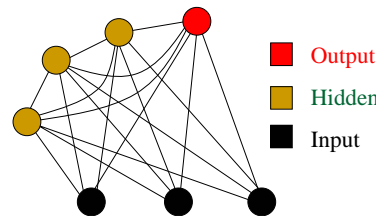


Power of compensated tremor = 0.902

The power of the tremor is reduced by 87.67%

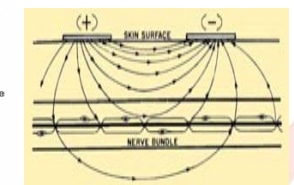
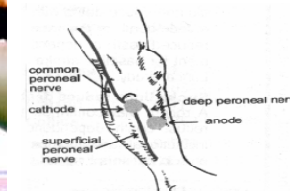
Tremor Filtering via ANN

- Cascade Correlation Neural Networks with extended Kalman Filtering
- Experiments with 11 multiple sclerosis patients (intention tremor)
- Smoother trajectory
- Reach and dwell in target circle 31.8% faster
 - Mean over 29 tests

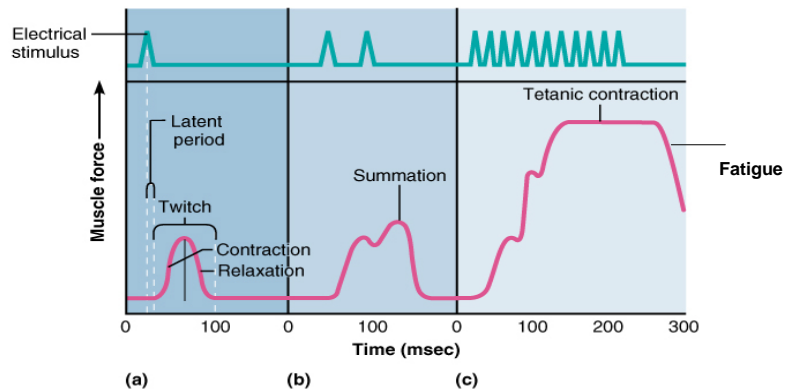


Functional Electrical Stimulations

- Controlling electrical pulses to stimulate the intact peripheral nerve to actuate muscles
 - Usually used to restore the motor functions for the paralyzed patients
- Prochazka *et al.* (1992) demonstrated the effectiveness of FES for tremor attenuation
 - Offline trial & error tuning of intensity and phase



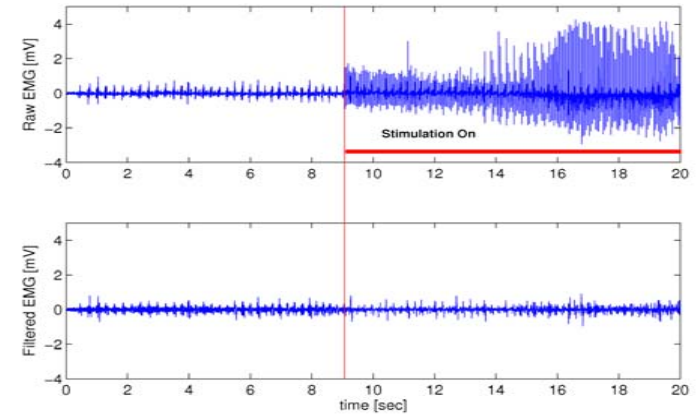
Muscle Activation



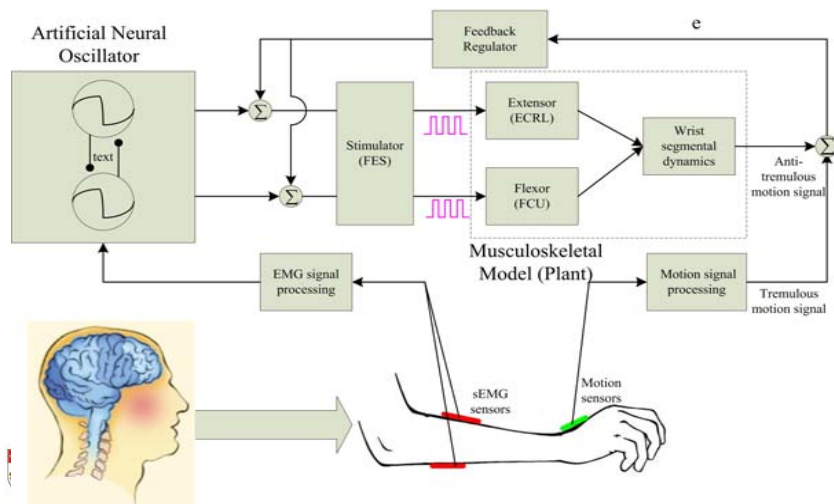
Stimulation Artifact

Blocking window

- Turn off EMG channels when stimulation is on

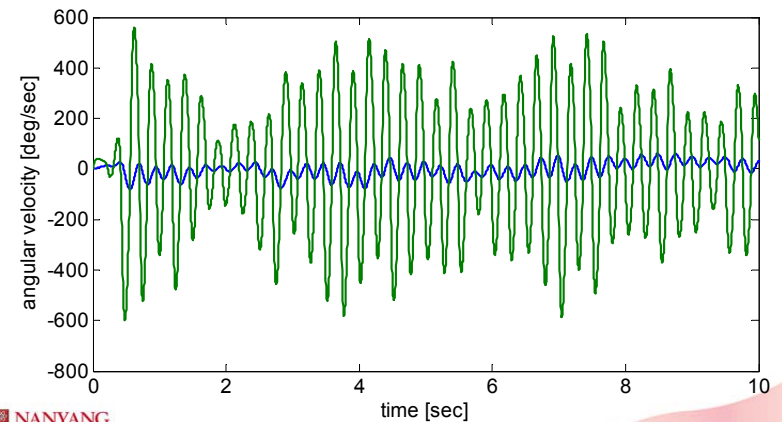


FES Controller Design



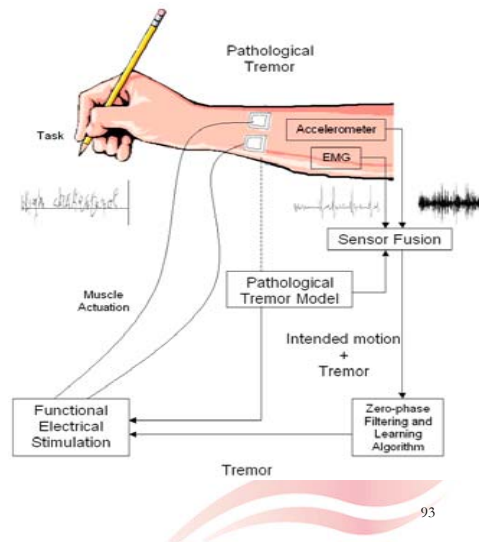
Simulation Result of Tremor Suppression

No ethical clearance on patient trial yet



Wearable Orthosis

- Wearable bands thin enough to be worn under sleeves
- Battery powered
- Microcontroller based
- Beyond the first step
 - False alarm
 - EEG



Questions & Comments

Wei Tech ANG

School of Mechanical & Aerospace Engineering

Nanyang Technological University

Singapore

wtang@ntu.edu.sg

<http://www.ntu.edu.sg/mae/centres/rrc/biorobotics/biorobotics.htm>